Title of document: **THERMAL ANALYSES AT MAMMOTH DIKE**

Client: **AGNICO EAGLE MINES LTD.**

Project: **WHALE TAIL WATER MANAGEMENT INFRASTRUCTURE DETAILED ENGINEERING**

Prepared by: Mathieu Durand-Jézéquel, Jr. Eng., M. Sc.

Reviewed by: Getahun Haile, P. Eng., M.Sc.A

Approved by: Yohan Jalbert, P. Eng.

REVISION INDEX

Revision				Pages Revised	Remarks
#	Prep.	App.	Date		
PA	MDJ		2018-04-30		
PB	GH/MO	YJ	2018-08-28	All	Issued for internal review
00	MDJ	YJ	2018-10-15	All	Final version

NOTICE TO READER

TABLE OF CONTENTS

List of figures

List of tables

1.0 Introduction

Agnico Eagle Mines Limited, Meadowbank Division ("Agnico Eagle") is developing the Whale Tail Pit project, a satellite gold deposit, as a continuation of current mine operations. The property is a 408 km² site located on Inuit Owned Land, approximately 150 km north of the Hamlet of Baker Lake and approximately 50 km northwest of the Meadowbank Mine in the Kivalliq region of Nunavut. The property, whose approximate location is shown on Figure 1-1, was acquired by Agnico Eagle in April 2013.

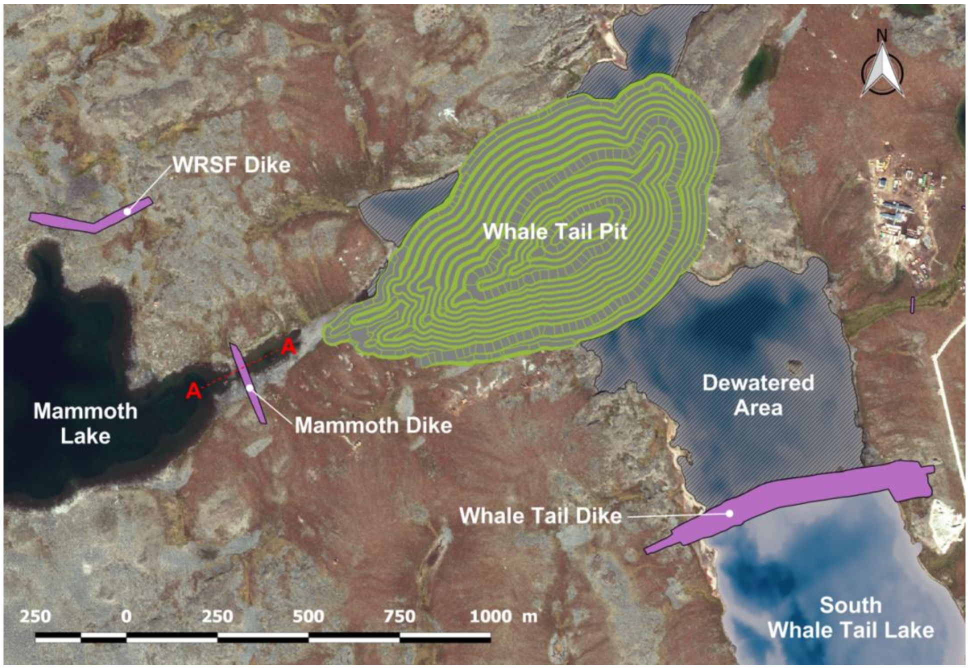

Figure 1-1: Mammoth dike general location

SNC-Lavalin was retained in September 2017 to develop the detailed engineering of the water management infrastructure. The current report documents one of three thermal analyses performed as part of the detailed engineering work of the Whale Tail project. The two other thermal analyses completed are for the Whale Tail Dike, which is the main dewatering embankment (SNC-Lavalin, 2018a) and for the Waste Rock Storage Facility dike (WRSF Dike) (SNC-Lavalin, 2018b). The thermal analyses report for the Whale Tail Dike is the most comprehensive of the three as it includes more detailed site specific information concerning field and laboratory geotechnical data. Mammoth Dike, to be built across the north-west finger of the lake with the same name, is the smallest of the three dikes mentioned above (Figure 1-2).

This report presents the available factual information, the thermal parameters and the methodology together with the main results of the analyses together with conclusions and recommendations.

The main objective of this study is to assess the long-term thermal regime of Mammoth Dike and its foundation over 50 years considering the operation of Whale Tail Pit project and its closure period during which Mammoth Dike may needs to stay operational.

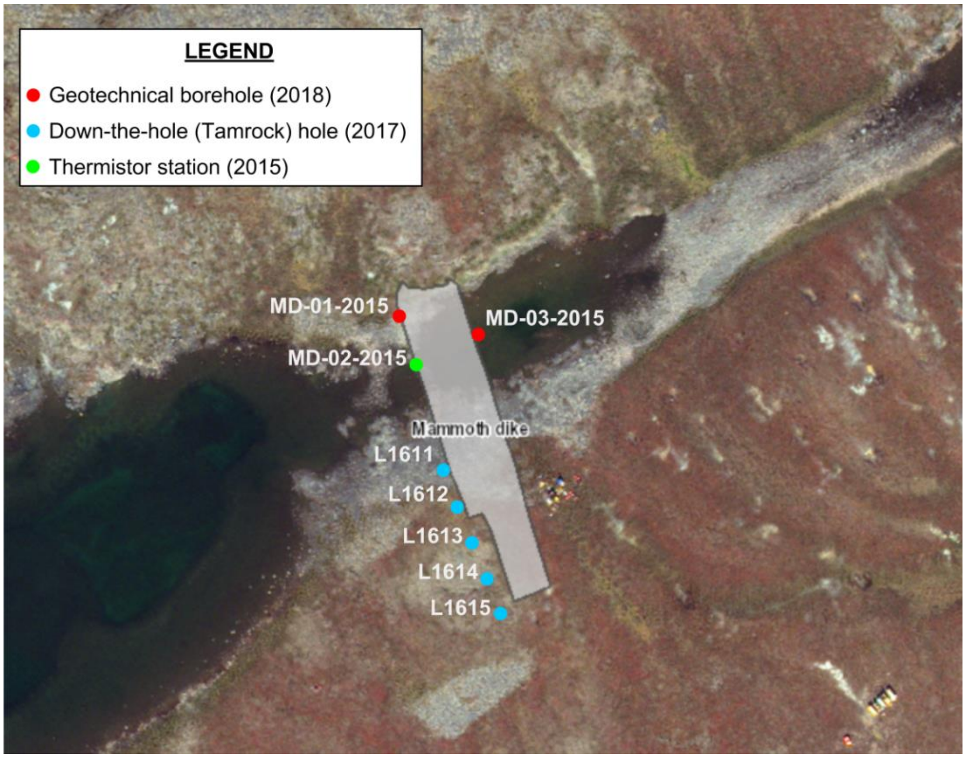

Figure 1-2: Mammoth dike geotechnical sounding locations and thermistor string station

2.0 Methodology

The thermal analyses were carried out using TEMP/W, a finite element computer program, a component of GeoStudio software suite (version 8.16.2.14053, GEO-SLOPE 2017). It can be used to model thermal changes in the ground by analyzing both simple and highly complex geothermal problems (GEO-SLOPE International Ltd., 2014).

2.1 Section Analyzed

The typical section shown on Figure 2-1, located about a third way from the north-west abutment and labelled as Section A-A on Figure 1-1 was selected for the thermal modeling. The dike is composed of rockfill lined on the upstream side with bituminous geomembrane (BGM). The BGM on the slope of the dike is keyed at the toe in a layer of fine filter amended with bentonite (FFAB). The material properties and boundary conditions used in the thermal modeling are discussed in subsequent sections of the report. It is important to note that the dike cross-section shown on Figure 2-1 is for a two-lane road for 150–ton haul trucks, which was being considered when the thermal model was first developed. The actual dike crest (road) shown on the design drawings is for a single lane. However, since the focus of the thermal analyses is the thermal regime of the FFAB, the model was maintained since it does not affect the results. It is also important to point out that section shown on Figure 2-1 is based on the preliminary design of the Mammoth Dike (SNC-Lavalin, 2017). However it is similar to the actual sections shown on the construction drawings.

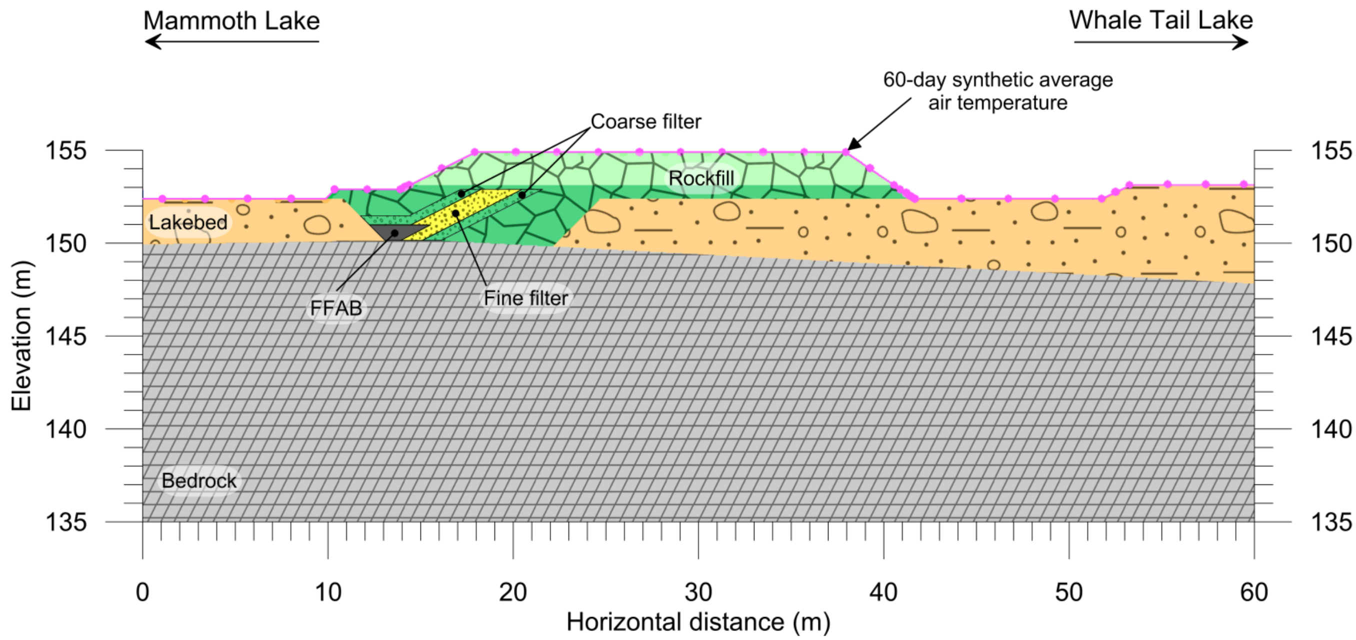

Figure 2-1: Cross section of Mammoth Dike modeled

2.2 Existing thermistor string

The only thermistor string that is within the footprint of Mammoth Dike, labelled MD-02-2015, is shown on Figure 1-2. The thermistor string, installed in May 2015, is located along the upstream toe of the dike. Figure 2-2A shows a photograph of the 13 m long thermistor-string, while Figure 2-2B provides the temperatures readings recorded between August 2017 and April 2018.

The photograph shown on Figure 2-2A was taken on September 2, 2015 looking west towards Mammoth Lake. The thermistor string is located in a boulder field underlain by approximately two metres of till. At the time of the thermistor reading, the water level was just above the lake bed. The temperature readings show that the active layer is around 4.5 metres deep and that the temperature in the bedrock stabilizes rapidly with depth. As could be expected, the depth of the active layer is higher than at other thermistors, located on land at the Whale mine site, on account of the presence of the water (though shallow) above the lake bed at the thermistor station.

2.3 Modeling Assumptions and Boundary Conditions

2.3.1 Air Temperature

There is no weather station at the Whale Tail site. The two nearest Environment Canada meteorological stations are located about 100 km from the Whale Tail project site: Back River (2300MQM) and Baker Lake A (2300503). However, for this mandate, it was assumed that the data collected at the Meadowbank weather station between 2012 and 2016 (Figure 2-3A), located approximately 50 km south of the project site, are representative for the purpose of the thermal analysis.

The mean annual air temperature (MAAT) for the 2012 to 2016 period is -11°C. A 365-day synthetic air temperature curve was computed from the 2012-2016 daily average. This approach implies averaging the daily air temperature for all five years recorded (Figure 2-3B).

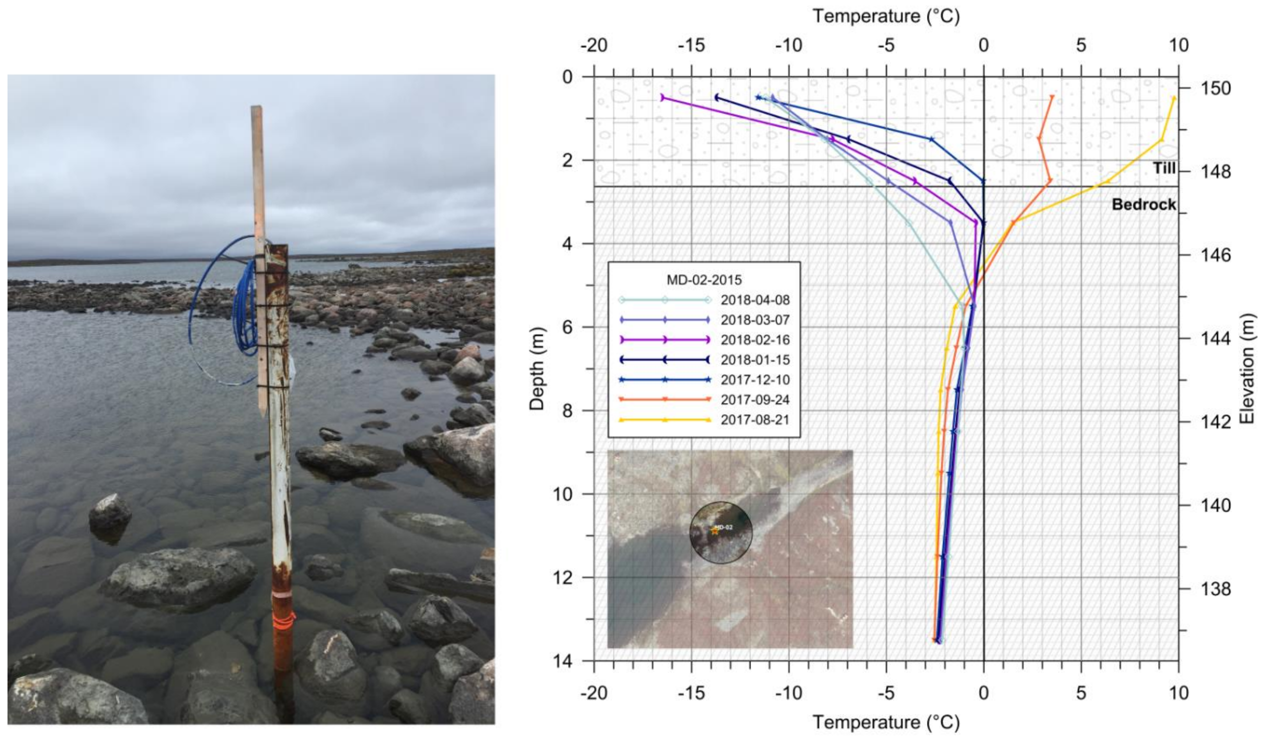

(A) (B)

Figure 2-2: Photograph of MD-02-2015 thermistor string by September 2015 (a) and temperature readings between August 2017 and March 2018 (b)

In order to simplify and accelerate the modeling process, the synthetic daily air temperature was converted to a synthetic 60-day average air temperature, reducing considerably the temperature data set. This 60-day average air temperature curve is plotted by using only the 2012-2016 daily average temperature every 60 days. Although the data accuracy is reduced, the general trend reflecting the annual variation in the air temperature is preserved (Figure 2-3B). This simplified 60-day synthetic air temperature curve was hence repeated periodically for the duration of the modeling.

2.3.2 Precipitations

It has been assumed that there is no significant snow accumulation that could affect the thermal regime of the model. The effect of precipitation and the impact of convective heat transfer could be included in the model by coupling the heat transfer regime with seepage, but it has not been taken into account in the present analyses.

2.3.3 Material Properties

Five distinct materials where used for the thermal analyses:

> Bedrock;
> Saturated and unsaturated fine filter;
> Saturated and unsaturated rockfill / coarse filter / lakebed material.

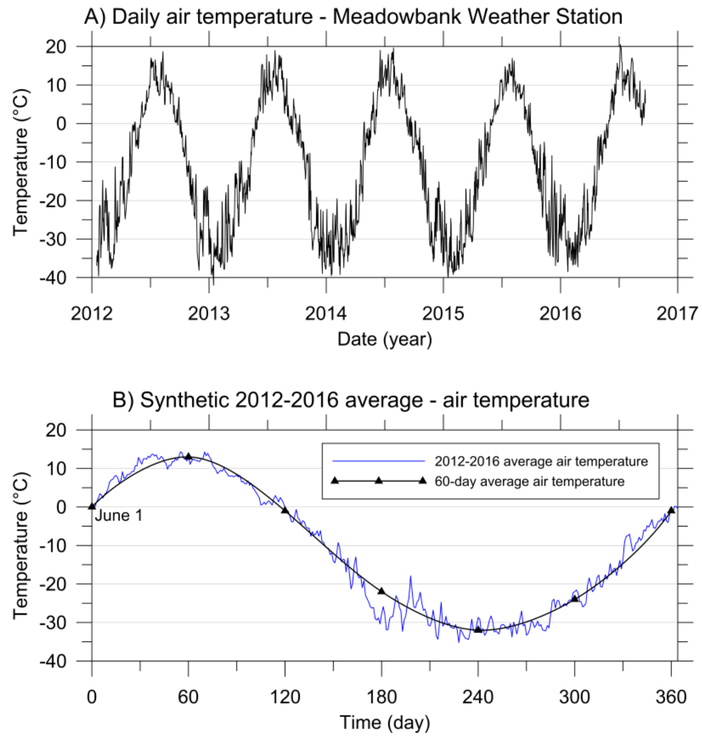

Figure 2-3: Air temperature curves

The geotechnical and thermal properties of the materials listed above are described in the thermal analyses report of the Whale Tail Dike (SNC-Lavalin, 2018a) and are also used for the analyses of Mammoth Dike with one exception as explained next. Since the lakebed foundation of Mammoth Dike is composed mostly of gravel, cobbles and boulders, it has been assigned the same geothermal properties as those selected for the rockfill and the coarse filter as summarized in Table 2-1.

2.3.4 Phase Change of Water – Freezing Point Depression

Freezing point depression is associated with a specific temperature where free water starts to freeze. For pure water, the freezing point is equal to 0°C. It can be affected by the salinity (total dissolved solids in the solution). For the present analyses the freezing point of water has been assigned 0 °C.

2.3.5 Surface n-factor

To simplify the thermal modeling (and due to limited field data), the air and ground surface temperatures were linked in the model with an estimated n-factor. Ground surface boundary conditions were correlated with the air temperature using an empirically determined n-factor. The freezing n-factor n_f corresponds to the ratio between the surface freezing index and the air freezing index, whereas the thawing n-factor n_t corresponds to the ratio between the surface thawing index and the air thawing index. The freezing index is the sum of negative degree-days over a given period (thawing index is the sum of positive degree-days). Those factors allow the ground surface temperature to be estimated from the air temperature dataset, which accounts for net radiation, vegetation, snow cover, ground thermal properties, surface relief, and subsurface drainage (Andersland & Ladanyi, 2004). The previous thermal analyses (SNC-Lavalin, 2017a; 2018) used empirical values of n_f = 1.0 and n_t = 1.3, based on trial and error simulations. These values have also been used in the present study as explained in Section 3.3.

Table 2-1: Physical and Thermal Properties of Materials Used For the Thermal Analyses

Layer	1 – Bedrock (Note 1)	2 – Saturated fine filter and FFAB (Note 2)	3 – Unsaturated fine filter	4 –Saturated rockfill / coarse filter / lakebed	5 - Unsaturated rockfill / coarse filter
Description	Undifferentiated foliated granitic rocks.	Poorly graded sand (SP).	Poorly graded sand (SP).	Crushed rock / Boulders, sandy gravel with some silt.	Crushed rock.
Geotechnical Parameter					
Dry density, ρ_d (kg/m³)	2667	2208	2208	2241	2241
Density of soil solids, ρ_s (kg/m³)	2710	2650	2650	2650	2650
Bulk density, ρ (kg/m³)	2683	2375	2284	2284	2263
Gravimetric water content, *w*	0.6 %	7.5 %	3.4 %	6.9 %	1.0 %
Volumetric water content, θ_w	1.6 %	16.7 %	7.5 %	15.4 %	2.2 %
Degree of saturation, S_r	100 %	100 %	45 %	100 %	15 %
Porosity, *n*	0.02	0.17	0.17	0.15	0.15
Void ratio, *e*	0.02	0.20	0.20	0.18	0.18
Specific surface area, S_s (m²/g)	6[a]	0	0	0	0
Geothermal Parameters					
Unfrozen thermal conductivity, k_u (kJ/day/m/°C)	211	171	138	173	119
Frozen thermal conductivity, k_f (kJ/day/m/°C)	216	213	116	212	108
Unfrozen Heat capacity, C_u (kJ/m³/°C)	2161	2365	1982	2338	1785
Frozen Heat capacity, C_f (kJ/m³/°C)	2124	1983	1810	1985	1734

Notes

1. Reference: Basalt (Anderson & Tice, 1972)
2. The geothermal properties of FFAB are considered the same to those of the saturated fine filter.

2.3.6 Geothermal Gradient

The previous thermal analyses (SNC-Lavalin, 2017a; 2018) used a geothermal gradient of 0.0217 °C/m. The same value was used in the current study.

2.3.7 Boundary Conditions

2.3.7.1 Upper surface boundary

In the steady-state analysis, the upper surface boundary corresponds to the mean annual ground temperature (MAGT) at the surface. The MAGT was calculated using the air temperature dataset, and by multiplying the values above 0 °C by n_t (1.3) and the values below 0 °C by n_f (1.0). Thus, by correlating the air temperature with the corresponding n-factor, the MAGT is estimated at -10.2 °C.

In the transient analysis, the synthetic 60-day average air temperature presented in Figure 2-3 was used. The air temperature values were converted to ground temperature values using a thermal modifier function (n-factors). The thermal function is a periodic function with a period of 365 days, repeated for the duration of the transient analysis.

2.3.7.2 Bottom of the model

A constant temperature of 0 °C was used as a boundary condition for the bottom of the model instead of a heat flux associated with the geothermal gradient. The elevation of 20 m for the 0°C constant temperature boundary condition was found empirically using the geothermal gradient and the MAGT at the surface.

2.3.7.3 Side of the model

Zero heat flux is imposed along the sides of the model to avoid errors in the temperature distribution near them.

2.3.7.4 Dike temperature

The initial temperature of the dike, which includes the rockfill and filters, is fixed at -20 °C. The surface boundary condition is applied to the whole dike for one day in the transient analysis, after which the boundary condition is removed. This allows simulating the thermal effect of the construction of the dike on the frozen overburden during winter. In this study, the dike is considered fully constructed by January 15 (with frozen materials at a temperature of -20 °C).

2.4 Calibration of the Model

The model was calibrated using the thermistor string MD-02-2015 located within the footprint of Mammoth Dike. The main goal of calibrating the model was to ensure that boundary conditions and thermal properties of the materials used in the model reflect what is observed in the field. The model is 200 m wide and 135 m high. The dimensions of the model in the current study are sufficient to allow the results not to be influenced by the size of the domain. Boundary effects are neglected since the main focus of the analyses is in the center of the model. The mesh size increases gradually from 3 m at the surface to 20 m on the sides and at the bottom of the model. When the dike is modeled, the mesh size of its components is reduced to 1 m. The geometry of the cross section of Mammoth Dike used for calibration of the material properties and boundary conditions are shown in Figure 2-4.

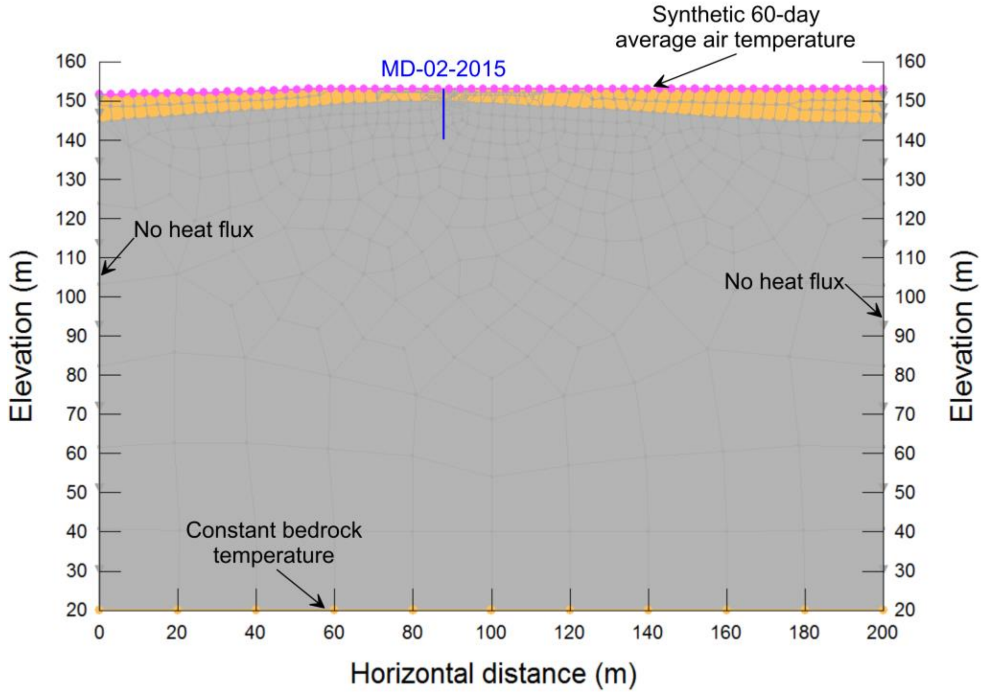

Figure 2-4: Geometry and boundary conditions Mammoth Dike thermal model

Using the boundary conditions described in section 2.3.7 and the thermal properties of the materials listed in Table 2-1, a steady-state analysis was carried out to establish the permanent thermal regime around Mammoth Dike. A 49-year transient analysis based on the initial conditions was then conducted to make sure that the steady-state results are replicated as close as possible. A 1-year transient analysis with a tight time step was finally performed to assess the annual variation of temperature at different depths in order to obtain the trumpet curve at the thermistor locations (Table 2-2).

Table 2-2: Modeling sequence for the calibration of the model

Modeling Sequence	Type of analyses	Duration	Time step	Saving increment	Parent analysis
Sequence 1 Calibration	Steady-State	-	-	-	-
Sequence 2 Initial conditions	Transient	49 years	5 days	50 days	Sequence 1 Calibration
Sequence 3 Initial conditions	Transient	1 year	1 day	1 day	Sequence 2 Initial conditions

If the observed data would fit within the annual variation of the model, it would mean good agreement between the thermal model and the field conditions. The thermal regime after 50 years and the range of annual ground temperature variations during the 50th year of transient analysis are shown in Figure 2-5.

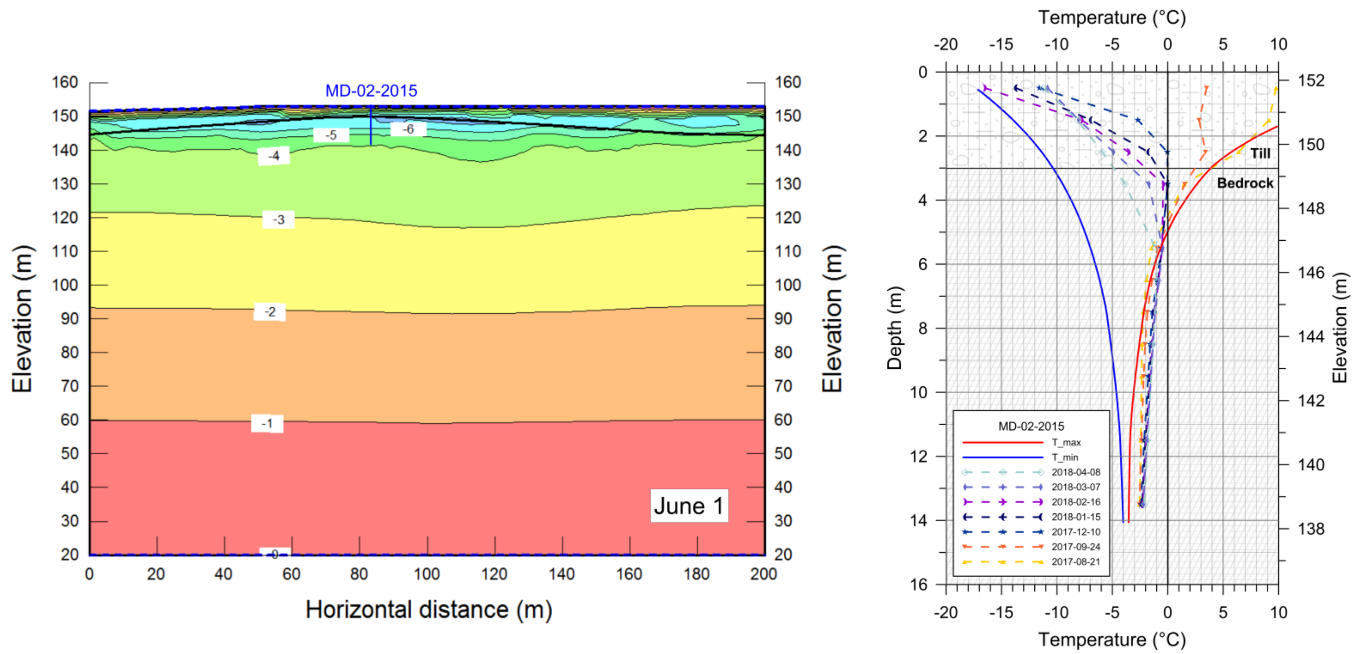

(A) (B)

Figure 2-5: Thermal regime at the mammoth dike area after 50 years of transient analyses (a) and comparison between annual ground temperature variation from the model and readings (b)

Figure 2-5A shows the spatial temperature distribution within the model by June 1, which is the result of thermal equilibrium between the constant temperature boundary condition at the bottom and synthetic average 2012-2016 air temperature boundary condition at the top. Figure 2-5B compares the maximum and minimum temperature curves obtained from the model with the actual readings from the MD-02-2015 thermistor string. The results show that the first five metres of the model replicate the field data reasonably well. In the permafrost zone (under the 5-metre active layer), the model shows that the maximum temperature profile is cooler by approximately 1 °C than the measured ones. The agreement between the model and the thermistor readings is better in the active zone than in permafrost. This is considered acceptable since the active zone is the main area of interest for the thermal analyses since it is the closest to where the FFAB layer will be constructed.

The calibration presented in Figure 2-5 was done using empirical n-factors of $n_\mathrm{f} = 0.6$ and $n_\mathrm{t} = 2.0$, which are different from the ones described in Section 2.3.5. In order to stay on the conservative side, the calibration of the whole model was done using thermistor string MD-02-2015. As shown on Figure 2-2A, this thermistor string is located in shallow water, which explains the warmer thermal regime at that location. Those n-factors gave the best fit while staying within the range of typical values for a gravel material (Lunardini, 1978; 1985). Knowing that the geothermal gradient is 0.0217 °C/m, the base of the permafrost at that location should be at a depth of 130 metres approximately.

For the rest of the simulations, the same n-factors than those used for the Whale Tail Dike thermal analysis ($n_\mathrm{f} = 1.0$ and $n_\mathrm{t} = 1.3$) were used because it is expected that they better simulate the actual thermal regime after the construction of Mammoth Dike. By applying the n-factors obtained from the calibration with MD-02-2015 to the whole model, the thermal regime was unrealistically too warm and would not represent the expected spatial distribution of temperature after construction of the dike.

3.0 Thermal Modeling

3.1 Main objective

The main objective of the thermal modeling of the cross section of Mammoth Dike is to understand the thermal regime of this infrastructure, especially that of the FFAB layer along the toe of the upstream slope of the dike in which the BGM will be anchored.

3.2 Geometry and Modeling Sequence

The geometry of the model is based on the cross section as shown in Figure 2-1. The details about the components of the dike and its geometry can be found in the technical note on the preliminary design of Mammoth Dike (SNC-Lavalin, 2017b). The safety berms were not considered in order to simplify the modeling process.

The model was first calibrated for the current field condition as described in Section 2.4. The 50 years of transient analyses for the calibration of the thermal model represent the last 50 years (1968-2018) assuming similar climatic conditions throughout the years. The beginning of the thermal analyses for the Mammoth Dike starts on June 1st, 2018 as indicated in Table 3-1.

Table 3-1: Modeling sequence for the thermal analysis at Mammoth Dike (see note)

#	Type of analysis	Approximate start date	Duration	Time step	Saving increment	Initial conditions
1	Transient	2018-06-01	228 days	1 day	1 day	50th year of transient analysis (calibration)
2*	Transient	2019-01-15	1 day	1 day	1 day	Analysis #1*(Note 1)
3	Transient	2019-01-16	136 days	1 day	1 day	Analysis #2
4	Transient	2019-06-01	4 years	5 days	30 days	Analysis #3
5	Transient	2023-06-01	365 days	1 day	1 day	Analysis #4
6	Transient	2024-06-01	14 years	5 days	30 days	Analysis #5
7	Transient	2038-06-01	365 days	1 day	1 day	Analysis #6
8	Transient	2039-06-01	29 years	5 days	30 days	Analysis #7
9	Transient	2068-06-01	365 days	1 day	1 day	Analysis #8

Note:

The modelling assumes that on January 15th, 2019, the construction of the Mammoth Dike is completed. The initial temperature of the dike is -20 °C as described in section 2.3.7.4.

The modeling sequence lasts 50 years after the construction of the dike, which makes it possible to assess the long term thermal regime of Mammoth Dike. A tighter saving increment after 5, 20 and 50 years of operation was used to evaluate the annual ground temperature amplitude. In order to simplify the modeling process, the upstream water level of Mammoth Lake was kept at a constant elevation of 152.73 m, which corresponds to the latest lake level recorded on June 26, 2018.

3.3 Modeling Results

Unlike the Whale Tail Dike, where following its construction, the upstream water level will rise by 3.5 m and the downstream side will be dewatered to allow open pit mining in the area, the construction of Mammoth Dike will not change significantly the ground thermal regime of the surrounding area. The dike was modeled assuming no ponded water above the FFAB due to the fact that based on the latest data, the lake level on June 26 m 2018 was at 152.73 m, thus below the lowest lake bed elevation of about 153 m as can be estimated on Figure 3-1. In addition, the same n-factors used for modeling of the east abutment of the Whale Tail Dike, namely a values of n_f=1.0 and n_t=1.3 were used (compared to n_f=0.6 and n_t=2.0 used to model the thermistor readings at the Mammoth dike which are located in shallow). The results show that the most noticeable effect of the construction of the embankment is to raise the permafrost table. This effect can be observed on Figure 3-2, which shows the thermal regime of Mammoth Dike after 50 years around October 15th, the time when the active layer is the deepest.

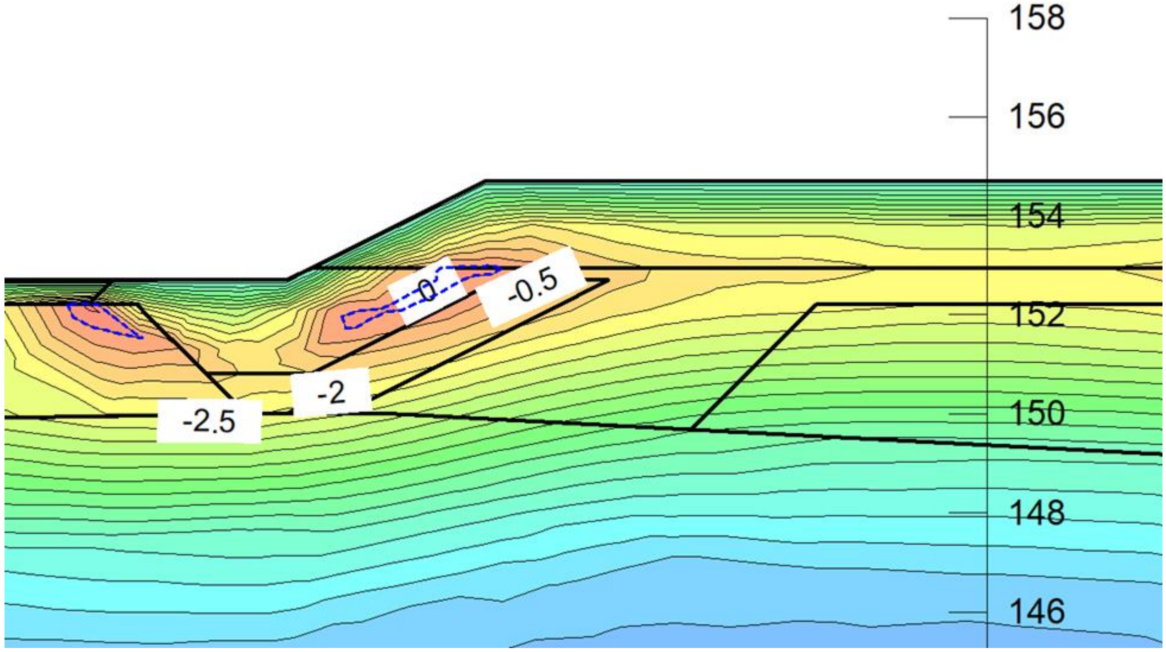

Figure 3-1: Thermal regime around the FFAB layer of Mammoth Dike in mid-October after 50 years

At the location of the FFAB, the temperature remains cool below about -1.5 ºC. This shows that the construction of Mammoth Dike causes the permafrost table to rise compared with the natural active layer depth on Figure 2-5B.

The main role of Mammoth Dike is to prevent flooding of the Whale Tail Pit. For the present study, significant rise in lake level and/or climate change with time were not taken into consideration.

3.4 Simple Mitigation Measure (if Required)

In the previous thermal analysis report for the Whale Tail Dike, SNC-Lavalin (2018) has demonstrated that the construction of an upstream “thermal berm” could be an option for preventing permafrost degradation on the upstream side of the dike due to the rise in the lake level. The thermal effect of extending the upstream crest of the rockfill embankment over the FFAB layer of Mammoth Dike was assessed as part of this study. The objective of this second thermal model was to evaluate the extent of permafrost rise above the FFAB layer by increasing the thickness of the rock fill above it.

The same modeling sequence as outlined in Table 3-1, as well as the same boundary conditions and material properties and n-factors were used as those for the dike without the upstream crest extension discussed in Section 3.3. The only change is in the geometry of the dike: the crest was extended upstream by approximately 6 m, allowing the entire FFAB layer to be overlain by about a 2 m thick additional layer of rockfill as can be seen on Figure 3-2, which also shows the thermal regime after 50 years.

The results of the analyses shown on Figure 3-1 confirm that the extension of the dike crest in the upstream direction will further lower the temperature of the FFAB to below about -3.0 ºC.

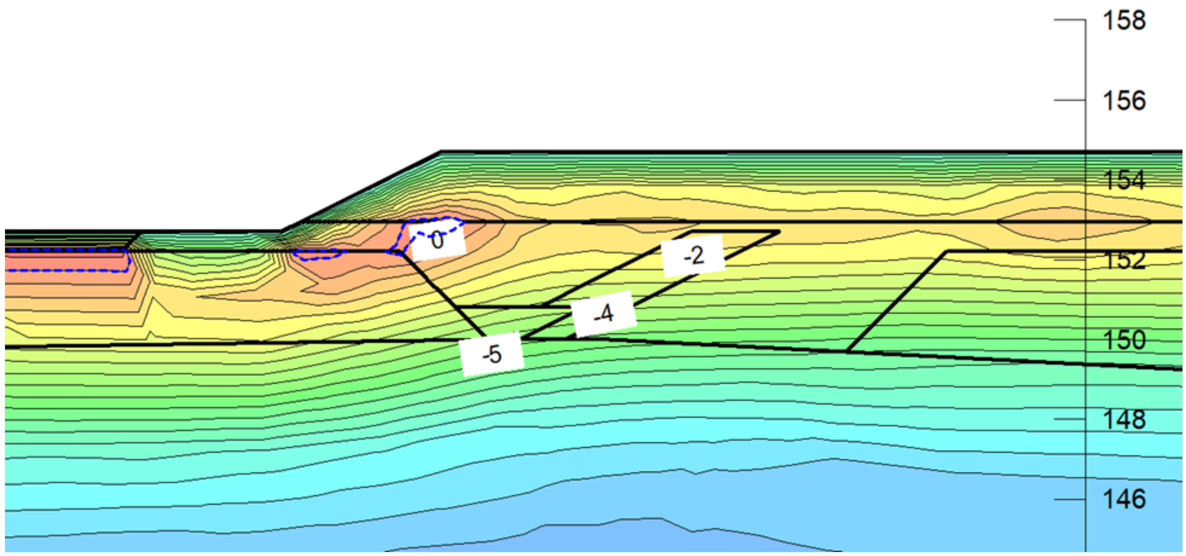

Figure 3-2: Thermal regime around the impervious zone of Mammoth Dike with the construction

4.0 Conclusions and Recommendations

4.1 Conclusions

Thermal analyses were carried out on a typical cross section of the Mammoth Dike in order to determine its thermal regime. The thermal model was calibrated using data from the thermistor string located within the footprint of the dike. Empirical n-factors were used to model the available factual data. The thermal effects of seepage and climate change were not taken into consideration in this study. Two models were analysed: first the dike cross section as shown on Figure 2-1 and a second one with same dike section but with the crest extended by about 6 m in the upstream direction to provide additional thermal cover to the FFAB.

The results of the thermal analyses show that:

- The FFAB of Mammoth Dike will remain in the frozen state at a temperature below -1.5 °C;
- Extension of the dike crest in the upstream direction by about 6 m and over the FFAB, will reduce the temperature of the FFAB by 1.5 °C down to below -3.0 °C.

4.2 Recommendations

Following the main conclusions drawn from the thermal analyses, the following recommendations can be made:

- Thermistor strings should be installed within the dike during its construction in order to monitor the thermal regime of the FFAB;
- If the data from the thermistor to be installed in the dike show that the FFAB is exposed to F-T cycles and/or significant seepage occurs in spring and summer, the dike crest could be extended in the upstream direction by about six (6) m to allow permafrost aggradation.

5.0 References

Andersland, O. B., & Ladanyi, B. (2004). *Frozen Ground Engineering - Second Edition.* John Wiley & Sons, 363 p.

Anderson, D. M., & Tice, A. R. (1972). Predicting unfrozen water contents in frozen soils from surface area measurements. *Frost Action in Soils* (pp. 12-18). Washington, D.C.: National Academy of Sciences.

GEO-SLOPE International Ltd. (2014). *Thermal modeling with TEMP/W: An Engineering Methodology.* September 2014 Edition.

Lunardini, V. J. (1978). Theory of n-factors and correlation of data. *Proc. 3rd Int. Conf. on Permafrost. 1*, pp. 41-46. Edmonton, Alberta: Ottawa: National Research Council of Canada.

Lunardini, V. J. (1985). Analytical methods for gound thermal regime calculations. In T. G. Krzewinski, & R. G. Tart Jr (Ed.), *Thermal Design Considerations in Frozen Ground Engineering* (pp. 204-257). New York: ASCE.

Smith, M., & Tice, A. (1988). Measurement of unfrozen water content of soils. In K. Senneset (Ed.), *Proc. 5th Int. Conf. on Permafrost* (pp. 473-477). Trondheim, Norway: Tapir, vol. 1.

SNC-Lavalin. (2017a). *Thermal analysis at Whale Tail Dike.* Report No. 640387-2000-4GER-0002, March 2017.

SNC-Lavalin. (2017b). *Preliminary design of Mammoth Dike.* 645003-3000-4GER-0001_01, August 2017.

SNC-Lavalin. (2018). *Thermal analysis at Whale Tail Dike.* Report No. 651298-2100-4GER-0001_PB, February 2018.